Progress In Electromagnetics Research M, Vol. 32, 57–72, 2013

RECONSTRUCTION OF MICROWAVE ABSORPTION OF MULTIPLE TUMORS IN HETEROGENEOUS TISSUE FOR MICROWAVE-INDUCED THERMO-ACOUSTIC TOMOGRAPHY

Jin-Guo Wang[1], Zhi-Qin Zhao[1, *], Jian Song[1], Zai-Ping Nie[1], and Qing-Huo Liu[2]

[1]School of Electronic Engineering, University of Electronic Science and Technology of China, Chengdu, Sichuan 611731, China

[2]Department of Electrical and Computer Engineering, Duke University, Durham, NC 27708, USA

Abstract—Time-of-flight (TOF) has been used to estimate sound velocity (SV) distribution of heterogeneous tissue to relieve the effect of acoustic heterogeneity in microwave-induced thermo-acoustic tomography (MITAT). Accurately picking the TOFs is significantly important to ensure high accuracy SV images, which greatly help to reconstruct the microwave absorption distribution accurately. However, current methods for picking the TOFs are designed for single source case. For breast tumor detection in MITAT, these methods become ineffective or even fail at the situation where multiple tumors are embedded in a normal breast tissue. In order to accurately reconstruct the microwave absorption properties of tumors in heterogeneous tissue in MITAT, an efficient method for picking tumors' TOFs is proposed. Combining the advantages of the wavelet transform and Akaike information criterion (AIC), the proposed method introduces a concept of separate extraction of TOFs. It can efficiently and accurately pick the TOFs of different tumors from the measured data in MITAT. Using the TOFs picked by the proposed method can efficiently help to reduce the effect of acoustic heterogeneity and greatly improve the accuracy and the image contrast of reconstructed microwave absorption properties. Some numerical simulations are given to demonstrate the effectiveness and feasibility of the proposed method in this paper.

Received 19 May 2012, Accepted 20 July 2013, Scheduled 24 July 2013

* Corresponding author: Zhi-Qin Zhao (zqzhao@uestc.edu.cn).

1. INTRODUCTION

Microwave-induced thermo-acoustic tomography (MITAT) has recently received much interest because of its great potential in detecting and diagnosing early-stage breast cancer [1–7]. In a MITAT system, the biological tissue is irradiated by a short electromagnetic pulse and then absorbs the microwave energy. Due to the dielectric differences among different biological tissues, microwave illumination will result in uneven heating for the tissues. Owing to the thermo-acoustic effect, the uneven heating gives rise to thermo-elastic expansion which radiates acoustic waves [1–7]. Because the microwave energy absorbed by tumor is much more than that by healthy adipose-dominated tissues [8], the tumor can be regarded as a thermo-acoustic source for breast cancer detection in MITAT. An image of the original acoustic pressure distribution, which reflects the microwave absorption properties of tissues, is reconstructed to detect tumor from the received acoustic waves [7]. Compared with microwave imaging and ultrasound imaging, MITAT exploits dielectric contrast at microwave frequencies while creates images with ultrasound resolution [8]. Therefore, MITAT combines the advantages of both microwave imaging and ultrasound imaging.

In MITAT, dense breast tissue often has unknown spatial variation in acoustic properties which must be taken into account in imaging [7, 9]. However, most current imaging methods neglect the effect of acoustic heterogeneity and assume the acoustic properties of tissue as homogeneous [9]. Due to the effect of acoustic heterogeneity of dense breast tissue, the reconstructed image of microwave absorption distribution will be blurred with the assumption of a homogeneous sound velocity (SV) distribution. In order to relieve the effect of acoustic heterogeneity, SV distribution must be estimated and utilized in the image reconstruction of original microwave absorption distribution [10–12]. In obtaining the SV distribution, time-of-flight (TOF) is a critical parameter. TOF is the time for the wave propagating through the medium from the thermo-acoustic source to the receiver. According to tumors' TOFs picked from the received data, the SV distribution can be iteratively updated by using an iterative reconstruction method [12] in MITAT. For this reason, accurately picking tumors' TOFs from the received ultrasonic signals is critical to ensure high accuracy SV distribution and therefore to accurately reconstruct the microwave absorption properties of tumors.

Various methods for picking the TOFs have been presented in literatures [13–17]. Among these methods, the W-AIC picker [17] has been widely used in many applications due to its robust performance.

However, not only the W-AIC method but also other current methods for picking the TOFs are designed for single source case. In MITAT, when two or more tumors exist in the biological tissue, they will produce ultrasonic signals simultaneously. For this situation, current methods can not accurately pick the TOFs for multiple tumors. Thus, the SV distribution of the biological tissues will be improperly estimated.

In order to solve the aforementioned problem, a new method for picking tumors' TOFs is developed in this paper. The proposed method introduces an idea of separate extraction to pick tumors' TOFs based on the W-AIC picker. The idea of separate extraction is that the ultrasonic signals induced by different tumors are firstly truncated from the received data by using different time windows. Then tumors' TOFs are picked separately by using W-AIC picker from the truncated signals. To summarize, the proposed method decomposes a multiple sources problem into several single source problems. With the TOFs picked by the proposed method, the image of microwave absorption properties of tumors is reconstructed by using an iterative reconstruction method [12]. Some simulation results demonstrate the effectiveness of the proposed method.

The remainder of the paper is organized as follows. In Section 2, a brief review on the iterative reconstruction method and the W-AIC picker is given. Then the proposed method is given and analyzed in Section 3. Some numerical results are shown in Section 4 to validate the proposed method. Conclusions are drawn in the last section.

2. A BRIEF REVIEW OF THE ITERATIVE RECONSTRUCTION METHOD AND W-AIC METHOD

2.1. Iterative Reconstruction Method

Aiming to reduce the effect of acoustic heterogeneity, an iterative reconstruction method (IRM) [12] has been proposed in MITAT. IRM consists of time reversal mirror (TRM) [18–21], fast marching method (FMM) and simultaneous algebraic reconstruction technique (SART) [10, 11]. It can reconstruct the microwave absorption properties of heterogeneous tissue using solely measured data with very few acceptable assumptions. The excellent performance of this algorithm has been demonstrated in [12]. The main idea of the IRM is shown in Fig. 1.

From Fig. 1, it can be seen that ΔTOF is a prerequisite in IRM because the initially assumed homogeneous SV is iteratively updated according to ΔTOF. Among the ΔTOF, TOF_{col}s which contain the information of real SV distribution are obtained from the measured

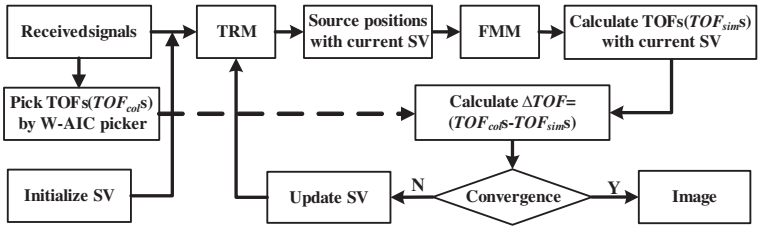

Figure 1. The block scheme of IRM.

data. Therefore picking tumors' TOFs (TOF_{col}s) from the measured data is a critical step in IRM. In IRM, the W-AIC picker is used to pick the TOF_{col}s. However, when there are two or more tumors existing in the breast tissue, the W-AIC picker can not accurately pick the TOFs of multiple sources. This may result in microwave absorption distribution of multiple sources reconstructed wrongly.

2.2. The W-AIC Picker

The W-AIC picker has been widely used in many applications due to its excellent performance in picking the TOFs. It combines the AIC picker with wavelet transform to improve the accuracy of picking the TOFs [17].

For a given signal S, it can be decomposed into the wavelet coefficients at several scales. The approximate wavelet coefficients are usually used to analyze the signal because they indicate the residuals of the signal after the high frequency components are removed [17]. Zhang et al. concluded that decomposing a signal into three scales is appropriate [17]. For these reasons, we suppose that the approximate wavelet coefficients of the signal S at three scales are S_1, S_2, and S_3 respectively. Then the AIC values at the three scales are calculated by

$$AIC_p(k) = k \cdot \log\{\mathrm{var}(S_p[1,k])\} + (N-k-1) \cdot \log\{\mathrm{var}(S_p[k+1,N])\}, \quad p = 1,2,3, \quad (1)$$

where N is the length of the time window and k the sample point ranged from 1 to N. var$(\cdot)$ denotes variance.

The AIC picker selects the point with the minimum AIC value as the candidate at each scale. If these three sample points are in close proximity to each other, the sample point at scale 2 is chosen as the TOF of the signal S. Hence, the W-AIC picker always chooses only one point with minimum AIC value as the TOF point even if there are multiple signals induced by different sources in the time window. This is the reason why the W-AIC picker fails to handle the situation for

picking tumors' TOFs when multiple acoustic sources are contained in a dense breast tissue in MITAT.

3. THE PROPOSED METHOD

To solve the problem described in Section 2 for picking tumors' TOFs in MITAT, a concept of separate extraction is introduced. The purpose of the separate extraction is to make ultrasonic signals induced by tumors exist in different time windows. Then the multiple sources case is converted into several single source cases which the W-AIC picker can solve.

[7] and [22] reported that the amplitude distortion caused by the heterogeneity effects is not severe in breast tissue and the peak values of the ultrasonic signals can be extracted with a high probability. Here we employ the peak searching method proposed in [7] to search the peaks of ultrasonic signals. Then the ultrasonic signals induced by multiple tumors are truncated from the received data by using time windows according to the corresponding time points of the searched positive peaks. A schematic flowchart of the proposed method is shown in Fig. 2.

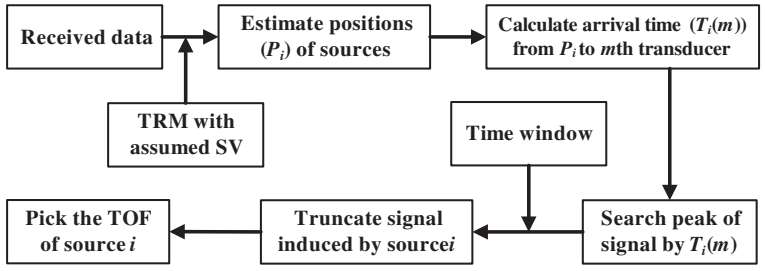

Figure 2. The flow chart of picking the TOFs of multiple tumors.

The process of the proposed method is summarized as:

1) Estimate the positions of tumors by using TRM with the assumption of homogeneous SV distribution. Assume there are N tumors in the tissue and note the estimated positions of tumors as P_i, $i = 1, \ldots, N$.
2) Calculate the arrival time $t_m(i)$ by using

$$t_m(i) = \frac{\|P_i - r_m\|}{v_0}, \quad i = 1, \ldots, N, \tag{2}$$

where r_m is the location of the mth transducer. v_0 is chosen to be the mean SV of tissue. $\|A\|$ denotes the Euclidean norm of A.

3) Search the positive peaks of the ultrasonic signals by using the following equation,

$$Peak_i = \max\left\{\max_{t\in[-\Delta_i,\Delta_i]}\{\tilde{s}_m(t), 0\}\right\}, \quad i = 1, \ldots, N, \tag{3}$$

where $\tilde{s}_m$ is the data received by the mth transducer. The searching range is $[-\Delta_i, \Delta_i]$ which is around the arrival time $t_m(i)$. Here Δ_i is a user parameter.

4) Find the time points corresponding to the searched peaks of the ultrasonic signals. Note the corresponding time points as TP_i, $i = 1, \ldots, N$.

5) Choose the interesting segments by using time windows (W_i, $i = 1, \ldots, N$):

$$W_i = [TP_i - \varepsilon \cdot D,\ TP_i + \varepsilon \cdot D], \quad \varepsilon = 0.5, \tag{4}$$

where D is the shortest distance from TP_i to TP_j, $j = 1, \ldots, N, j \neq i$.

6) Pick the TOFs using W-AIC picker from the truncated segments.

In steps 1) and 2), TRM technique is applied to estimate the positions of the acoustic sources because TRM seems to be the leading candidate as a generally applicable and robust imaging algorithm [18–21]. In MITAT, the real SV distribution of the biological tissue is unknown, but the spatially-averaged SV value of the tissue is usually known [7, 9]. Therefore, the SV distribution of the breast tissue is usually assumed as homogeneous [7, 9]. This is the reason why v_0 in (2) is chosen as the average SV value of tissue. So the positions of the acoustic sources is approximately reconstructed based on the assumed homogeneous SV distribution by using TRM. However, if two tumors are most closely located, then they are not resolved and reconstructed as one tumor. So according to our numerous simulations, when the distance between tumors is less than 1 cm, the proposed method will not resolve them.

Once the TOFs of multiple tumors are obtained, IRM is used to reconstruct the microwave absorption distribution of tumors.

4. NUMERICAL SIMULATIONS

In this section, the performance of the proposed method is validated through two examples: tumors embedded in fatty tissue and glandular tissue. In the first example, only tumors are the acoustic sources which radiate the ultrasonic signals. While in the second example, both tumors and glandular tissue are the acoustic sources. Furthermore,

in order to simulate realistic scenarios, Gaussian noise is added into the received signals. In [13], 18 dB of signal to noise ratio (SNR) *in vivo* breast data is regarded as low SNR. In the following examples, lower SNR (10 dB) is considered to test the performance of proposed method.

4.1. Tumors Embedded in Fatty Tissue (Example 1)

A 2-D breast model is shown in Fig. 3. The SV distributions of tissue 1–4 and the fat are modeled as 2-D Gaussian distribution with the standard deviation of 10 and the corresponding spatially-averaged SV values are set according to [10–12] and listed in Table 1. The breast tissue is put into the mineral oil which has permittivity similar to that of the fatty tissue [7]. The density of tissue is selected as $\rho = 0.893 * \mathrm{SV} - 349$, which is a relation derived from the measured properties of soft tissue [23].

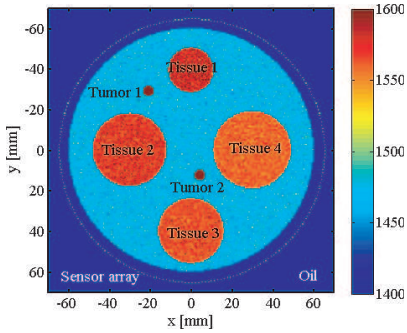

Figure 3. 2-D dense breast model.

Table 1. Sound velocities of different breast tissues.

Tissues	Fatty	Tissue 1	Tissue 2	Tissue 3	Tissue 4
Velocity (m/s)	1470	1580	1572	1560	1566

In [7, 24], the dielectric properties of fatty and tumor tissues are listed in Table 2. In MITAT, the specific absorption rate (SAR) distribution which is used as the acoustic pressure source is given as [7, 25]:

$$\mathrm{SAR}(r) = \frac{\sigma(r)E^2(r)}{2\rho(r)}, \tag{5}$$

where $\sigma(r)$ is the conductivity of the biological tissue at location r, $E(r)$ the electric field at location r, and ρ the density of the biological tissue. Assume electric field $E(r)$ is equal in the breast tissue, we can conclude that the acoustic pressure intensity of tumor is about 10 times larger than that of fat tissues from (5). Hence, two 5-mm-diameter tumors are assumed as the acoustic sources and the other four tissues do not emit acoustic signals [12]. The ultrasonic signals induced by two sources are simulated by using pseudo-spectral time-domain (PSTD) method [26]. 256 transducers are uniformly located on a circle surrounding the breast tissue to receive the data [10–12]. The grid-cell size used by PSTD is $0.5\,\text{mm} \times 0.5\,\text{mm}$ and the computational domain is divided into 256×256 grids in the simulations. To avoid artificial reflections caused by the truncation of the computational domain, perfectly matched layer (PML) absorbing boundary condition is induced.

Table 2. Dielectric properties of fatty and tumor tissues.

Tissues	Dielectric properties	
	Permittivity (F/m)	Conductivity (S/m)
Fatty tissue	9	0.4
Tumor	50	4

Figure 4(a) gives the TOFs picked by the proposed method and the W-AIC method when SNR is 10 dB. The solid line with triangles is the TOFs picked by the W-AIC method. The dashed lines with squares and points are the TOFs of tumor 1 and tumor 2 picked by the proposed method. Figs. 4(b) and (c) are the comparisons between the TOFs picked by the proposed method and the corresponding theoretical values. In Fig. 4(b), the solid line with squares is the TOFs of tumor 1 picked by the proposed method and the dashed line is the theoretical TOFs of tumor 1. In Fig. 4(c), the solid line with circles is the TOFs of tumor 2 picked by the proposed method and the dashed line is the theoretical TOFs of tumor 2. Fig. 4(d) plots the TOFs picked by proposed method and W-AIC at one receiver. The red point is the TOF picked by W-AIC and two green squares are the TOFs picked by proposed method. According to the results, we can conclude that the effect of the noise to the proposed method is small. This is because that the proposed method is based on the robust W-AIC picker, which has the ability for noise reduction. Therefore, the proposed method works well at low SNR in MITAT.

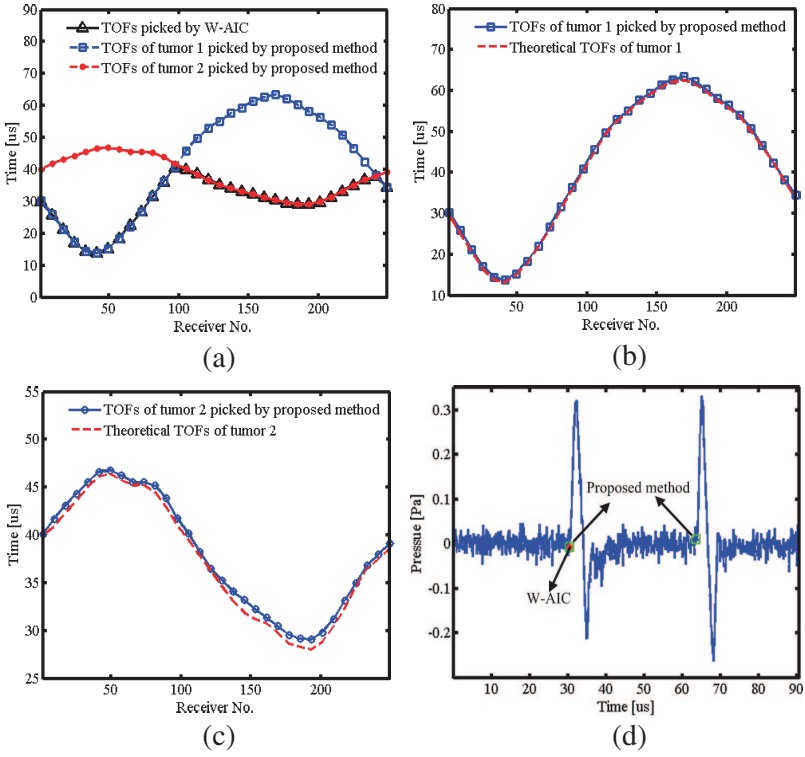

Figure 4. (a) TOFs picked by proposed method and W-AIC at SNR = 10 dB; (b) TOFs of tumor 1 picked by proposed method and corresponding theoretical TOFs; (c) TOFs of tumor 2 picked by proposed method and corresponding theoretical TOFs. (d) TOFs picked by proposed method and W-AIC at one receiver.

Figure 5(a) gives the microwave absorption distribution reconstructed by using TRM under the assumed homogeneous SV distribution and Gaussian noise. Two tumors are blurred and have low image contrast especially for tumor 2. Fig. 5(b) is the microwave absorption distribution reconstructed by IRM with the TOFs picked by W-AIC picker. Obviously in Fig. 5(b), only tumor 1 is recovered, while tumor 2 is missed, though tumor 1 has good agreement with the actual tumor size and location. According to the TOFs picked by the proposed method, the final microwave absorption distribution is given in Fig. 5(c). Both tumor targets are recovered and have much better spatial resolution and image contrast than Figs. 5(a) and (b). Compared with Fig. 5, noise has little effect to the final microwave absorption

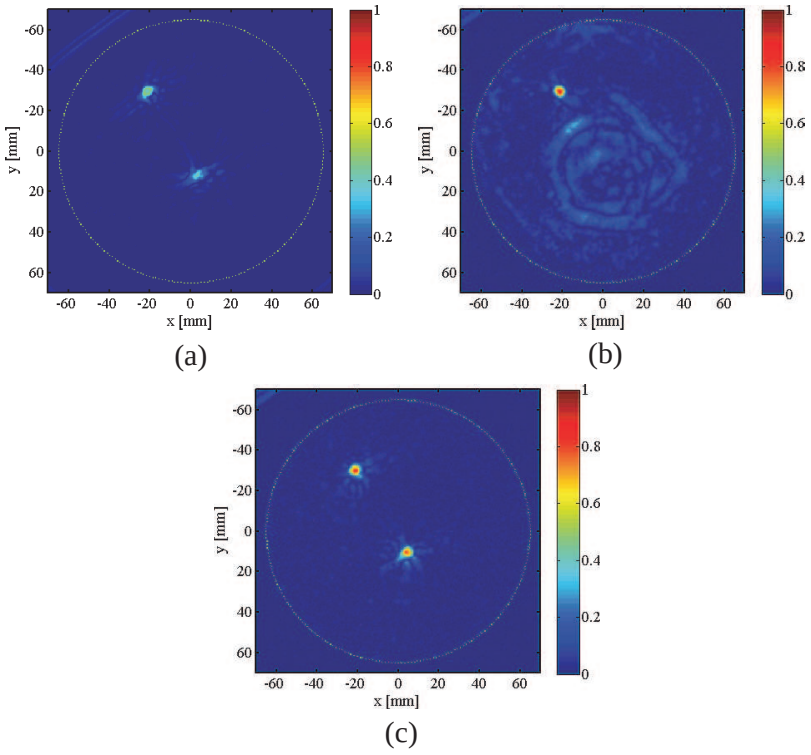

Figure 5. (a) Microwave absorption reconstructed by TRM; (b) Microwave absorption reconstructed by IRM with TOFs picked by W-AIC; (c) Microwave absorption distribution reconstructed by IRM with TOFs picked by proposed method.

reconstruction. Because the IRM involves the TRM engine, it also has the ability of noise reduction [20–24]. Moreover, Figs. 5(a)–(c) are all normalized.

In this example, the proposed method is validated when tumors are embedded in the fatty tissue. Compared with the W-AIC picker, the proposed method can efficiently and accurately pick the TOFs of both tumors while the W-AIC only picks a part of tumors' TOFs.

4.2. Tumors Embedded in Glandular Tissue (Example 2)

In this subsection, another example which considers the effect of normal glandular tissue is presented. Fig. 6 gives the specific configuration of 2-D breast model which refers to the dense breast

phantom in the UWCEM Numerical Breast Phantom Repository (http://uwcem.ece.wisc.edu) [27, 28]. In this model, the shape of normal glandular tissue is simplified as ellipse and the SV value of glandular tissue is 1540 m/s and other SV parameters are the same as previous example.

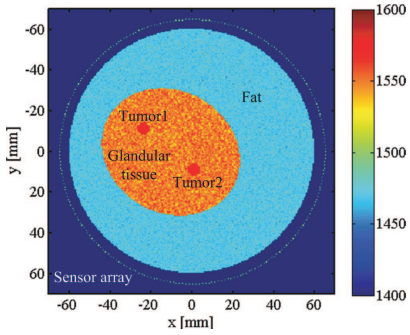

Figure 6. 2-D breast model with two tumors embedded in normal glandular tissue.

By referring to [8], the dielectric properties of different breast tissues are listed in Table 3. According to (5), SAR of both tumors and glandular tissue are much larger than that of fatty tissue. So, the effect of fatty tissue can be neglected and both tumors and glandular tissue are assumed as acoustic pressure sources in this simulations.

Table 3. Dielectric properties of different breast tissues.

Tissues	Dielectric properties	
	Permittivity (F/m)	Conductivity (S/m)
Fatty tissue	6.19	0.4
Glandular tissue	46.13	2.4
Tumor	49.78	4.8

Figure 7 gives the comparisons between different TOFs when Gaussian noise is added. In Fig. 7, the green triangular solid line is the TOFs picked by the W-AIC method. These picked TOF points are the TOFs of signals induced by glandular tissue. This is because that the ultrasonic signals induced by normal glandular tissue arrive at the receivers earlier than those of tumors. So the TOFs of two tumors can not be picked by using the W-AIC method. The blue solid line

and the black solid line with dots are the TOFs of tumors 1 and 2 picked by the proposed method. The corresponding theoretical values of TOFs for two tumors are marked in red dashed and dash-dotted lines, respectively. Comparing the TOFs picked by proposed method with the corresponding theoretical values, the relative errors of tumor 1 are below 9.6% and those of tumor 2 are below 6.1%. By using the proposed method, the TOFs of both tumors are efficiently picked while the W-AIC method only picks the TOFs of glandular tissue.

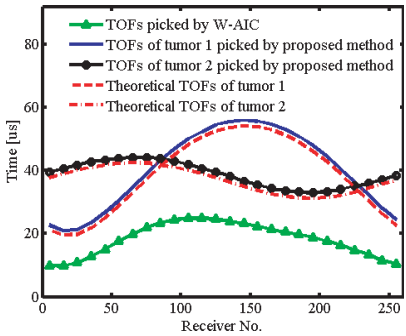

Figure 7. A comparison between different TOFs when SNR is 10 dB.

Figure 8 shows the reconstructed images in a given Gaussian noise environment. In Fig. 8, the red circles are the actual contours of tumors. Fig. 8(a) gives the microwave absorption distribution reconstructed by using TRM with assumed homogeneous SV distribution. From Fig. 8(a), tumors and normal glandular tissue are imaged. However, due to the effect of acoustic heterogeneity, tumors and glandular tissue are not accurately reconstructed. Both two tumors are blurred and have low image contrast. Since the TOFs of two tumors are wrongly picked by W-AIC, the SV distribution is estimated improperly and therefore the microwave absorption distribution of tumors is unfaithful. Fig. 8(b) shows the microwave absorption distribution reconstructed by using IRM with the TOFs picked by the proposed method. Both tumors and glandular tissue have good agreement with the actual tumor sizes and locations. Compared with Fig. 8(a), two tumors have much better spatial resolution and image contrast.

In this section, the feasibility of the proposed method has been validated through two examples. Compared with the W-AIC picker, the proposed method can efficiently and accurately pick the tumors' TOFs. This provides a guarantee for reconstructing the SV distribution. Thus it greatly improves the quality of the reconstructed

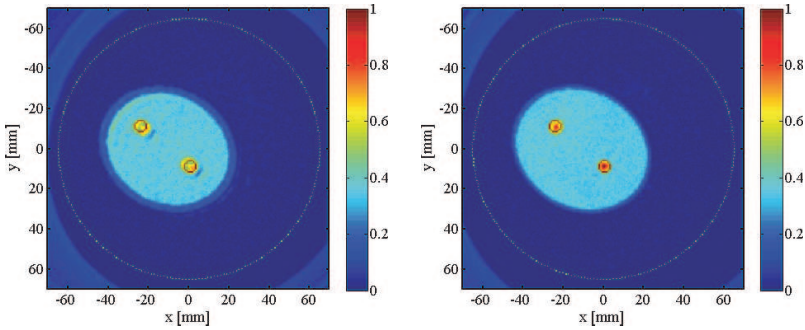

Figure 8. (a) Microwave absorption properties reconstructed by TRM with initially assumed SV distribution and Gaussian noise; (b) Microwave absorption properties distribution reconstructed by iterative reconstruction method with TOFs picked by proposed method and Gaussian noise.

image. Furthermore, the proposed method still works for 3D case in theory. However, the received data in 3D is large which results in huge computational cost. So some accelerating method [29] should be considered and utilized in 3D reconstruction.

5. CONCLUSIONS

In this paper, we propose an automatic TOF picker for multiple tumors in MITAT. The proposed method combines the W-AIC picker and induces an idea of separate extraction of TOFs. By using different time windows, ultrasonic signals induced by multiple tumors are separated. Then the TOFs of ultrasonic signals are extracted by using the W-AIC picker. The proposed method decomposes the problem of multiple sources into several single source problems. The efficiency and accuracy of the proposed method are demonstrated through two simulation examples. Moreover, it is also demonstrated that using the TOFs picked by proposed method can greatly improve the accuracy of reconstructed microwave absorption properties of dense breast tissue and the image contrast of tumors in MITAT system.

ACKNOWLEDGMENT

This research is supported by China NSFC (No. 60927002, No. 61171044, and No. 61231001).

REFERENCES

1. Omar, M., S. Kellnberger, G. Sergiadis, D. Razansky, and V. Ntziachristos, "Near-field thermoacoustic imaging with transmission line pulsers," *Med. Phys.*, Vol. 39, No. 7, 4460–4466, 2012.
2. Ku, G., B. D. Fomage, X. Jin, M. Xu, K. K. Hunt, and L. V. Wang, "Thermoacoustic and photoacoustic tomography of thick biological tissues toward breast imaging," *Technol. Cancer Res. Treat.*, Vol. 4, No. 5, 1–7, 2005.
3. Kruger, R. A., P. Liu, Y. R. Fang, and C. R. Appledorn, "Photoacoustic ultrasound (PAUS) — Reconstruction tomography," *Med. Phys.*, Vol. 22, No. 10, 1605–1609, 1995.
4. Ku, G. and L. V. Wang, "Scanning microwave-induced thermoacoustic tomography: Signal, resolution and contrast," *Med. Phys.*, Vol. 28, No. 1, 4–10, 2001.
5. Zeng, X. and G. Wang, "Numerical study of microwave-induced thermo-acoustic effect for early breast cancer detection," *IEEE Antennas and Propagation Society International Symposium*, 839–842, 2005.
6. Xu, M. and L. V. Wang, "Pulsed-microwave-induced thermoacoustic tomography: Filtered backprojection in a circular measurement configuration," *Med. Phys.*, Vol. 29, No. 8, 1661–1669, 2002.
7. Xie, Y., B. Guo, J. Li, G. Ku and L. V. Wang, "Adaptive and robust methods of reconstruction (ARMOR) for thermoacoustic tomography," *IEEE Trans. Biomed. Eng.*, Vol. 55, No. 12, 2741–2752, 2008.
8. Lazebnik, M., D. Popovic, L. M. Cartney, et al, "A large-scale study of the ultrawideband microwave dielectric properties of normal, benign and malignant breast tissues obtained from cancer surgeries," *Phys. Med. Biol.*, Vol. 52, No. 20, 6093–6115, 2007.
9. Cox, B. T. and B. E. Treeby, "Artifact trapping during time reversal photoacoustic imaging for acoustically heterogeneous media," *IEEE Trans. Med. Imag.*, Vol. 29, No. 2, 387–396, 2010.
10. Li, S., M. Jackowski, D. Dione, L. Staib, and K. Mueller, "Refraction corrected transmission ultrasound computed tomography for application in breast imaging," *Med. Phys.*, Vol. 37, No. 5, 2233–2246, 2010.
11. Li, S., K. Mueller, M. Jackowski, D. Dione, and L. Staib, "Fast marching method to correct for refraction in ultrasound computed tomography," *IEEE International Symposium in Biomedical*

Imaging (ISBI), 896–899, 2006.

12. Wang, J. G., Z. Q. Zhao, J. Song, X. Zhu, Z. P. Nie, and Q. H. Liu, "Reconstruction of microwave absorption properties in heterogeneous tissue for microwave-induced thermo-acoustic tomography," *Progress In Electromagnetics Research*, Vol. 130, 225–240, 2012.
13. Li, C., L. Huang, N. Duric, H. Zhang, and C. Rowe, "An improved automatic time-of-flight picker for medical ultrasound tomography," *Ultrasonics*, Vol. 49, No. 1, 61–72, 2009.
14. Molyneux, J. B. and D. R. Schmitt, "First-break timing: Arrival onset times by direct correlation," *Geophysics*, Vol. 64, No. 5, 1492–1501, 1999.
15. Boschetti, F., D. Dentith, and R. D. List, "A fractal-based algorithm for detecting first-arrivals on seismic traces," *Geophysics*, Vol. 61, No. 4, 1095–1102, 1996.
16. Sleeman, R. and T. Eck, "Robust automatic P-phase picking: An on-line implementation in the analysis of broadband seismogram recordings," *Phys. Earth Planet Interiors*, Vol. 113, Nos. 1–4, 265–272, 1999.
17. Zhang. H., C. Thurber, and C. Rowe, "Automatic P-wave arrival detection and picking with multiscale wavelet analysis for single-component recordings," *Bull. Seism. Soc. Am.*, Vol. 93, No. 5, 1904–1912, 2003.
18. Fink, M. and C. Prada, "Acoustic time reversal mirror," *Inv. Probl.*, Vol. 17, No. 1, 1–38, 2001.
19. Xu, Y. and L. V. Wang, "Time reversal and its application to tomography with diffracting sources," *Phys. Rev. Lett.*, Vol. 92, No. 3, 1–4, 2004.
20. Chen, G. P., W. B. Yu, Z. Q. Zhao, Z. P. Nie, and Q. H. Liu, "The prototype of microwave-induced thermo-acoustic tomography imaging by time reversal mirror," *Journal of Electromagnetic Waves and Applications*, Vol. 22, Nos. 11–12, 1565–1574, 2008.
21. Chen, G. P., Z. Q. Zhao, Z. P. Nie, and Q. H. Liu, "A computational study of time reversal mirror technique for microwave-induced thermo-acoustic tomography," *Journal of Electromagnetic Waves and Applications*, Vol. 22, No. 16, 2191–2204, 2008.
22. Xu, Y. and L. V. Wang, "Effects of acoustic heterogeneity in breast thermoacoustic tomography," *IEEE Trans. Ultrasonic, Ferroelectrics, Frequency Control*, Vol. 50, No. 9, 1134–1146, 2003.
23. Mast, T. D., "Empirical relationship between acoustic parameters

in human soft tissue," *Acoust. Res. Lett.*, Vol. 1, No. 2, 37–42, 2000.

24. Guo, B., Y. Wang, J. Li, P. Stoica, and R. Wu, "Microwave imaging via adaptive beamforming methods for breast cancer detection," *Journal of Electromagnetic Waves and Applications*, Vol. 20, No. 1, 53–63, 2006.
25. Bernardi, P., M. Cavagnaro, S. Pisa, and E. Piuzzi, "SAR distribution and temperature increase in an anatomical model of the human eye exposed to the field radiated by the user antenna in a wireless LAN," *IEEE Trans. Microw. Theory Tech.*, Vol. 46, 2074–2082, 1998.
26. Liu, Q. H., "The pseudospectral time-domain (PSTD) algorithm for acoustic waves in absorptive media," *IEEE Trans. Ultrasonics, Ferroelectrics and Frequency Control*, Vol. 45, No. 4, 1044–1055, 1998.
27. Mashal, A., J. H. Booske, and S. C. Hagness, "Towards contrast-enhanced microwave-induced thermoacoustic imaging of breast cancer: An experimental study of the effects of microbubbles on simple thermoacoustic targets," *Phys. Med. Biol.*, Vol. 54, No. 3, 641–650, 2009.
28. Zastrow, E., S. K. Davis, and S. C. Hagness, "Safety assessment of breast cancer detection via ultrawideband microwave radar operating in pulsed-radiation mode," *Microw. Opt. Technol. Lett.*, Vol. 49, No. 1, 221–225, 2007.
29. Capozzoli, A., C. Curcio, and A. Liseno, "GPU-based ω-K tomographic processing by 1D non-uniform FFTs," *Progress In Electromagnetics Research M*, Vol. 23, 279–298, 2012.